U.S. Department of the Interior

U.S. Geological Survey

X-ray mineralogy of sediments from the southern Black Sea and selected rivers

by

Lawrence J. Poppe[1] and Bernward J. Hay[2]

Open-File Report 93-274

[1]USGS, Woods Hole, Massachusetts 02543
[2]Louis Berger and Assoc., Waltham, Massachusetts 02154

ABSTRACT

X-ray powder diffraction analyses were performed on sediment samples from 16 cores collected in the southern Black Sea and from 9 adjacent rivers. The results of these analyses show that provenance controls the distribution of detrital sediments in the Black sea. Illite dominates the mineralogy of the clay fraction in the rivers that discharge into the western part of the Black Sea and, consequently, the mineralogy of the Holocene bottom sediments in the southwestern basin of the Black Sea. Conversely, smectite dominates the mineralogy of the clay fraction in the rivers of north-central Turkey and, consequently, the mineralogy of the Holocene bottom sediments in the southeastern basin of the Black Sea. Variations in the environment have resulted in changes in the sediment supply and eustatic sea level and have dramatically altered the sediment distribution patterns through time.

INTRODUCTION

During April-May 1988, 62 gravity cores and 30 box cores were collected aboard the R/V Knorr (Honjo and Hay, 1988). The focus of this cruise was to study sediment variability throughout the anoxic history of the Black Sea with high spatial and temporal resolution.

Most of the cores collected from the deepwater (>1,000 m) areas of the Black Sea have penetrated three distinct units (Ross and others, 1970; Shimkus and Trimonis, 1974). The uppermost unit (Unit 1) is about 30 cm (26-78 cm) thick and is characterized by microlaminations that occur at a rate of about 50-100/cm. The darker, more organic-rich layers are interspaced with lighter, more carbonate-rich layers composed largely of coccolithophorids. The middle unit (Unit 2) is a 20-45 cm thick sapropel that consists of very finely laminated, dark olive gray to black organic-rich clay. Earlier estimates of the number of varves in this sapropel (Honjo and Hay, 1988) suggest that this unit represents a duration of about 4,500 years. The lowermost unit (Unit 3) is composed of homogeneous to burrow-mottled black, gray, and greenish gray clay. None of the cores penetrated the base of this lowermost unit.

The pelagic sedimentation recorded in these units is usually interrupted by at least one or more fine-grained turbidites. These turbidites are largely responsible for the variations in thickness of the units.

This sequence of units is interpreted to represent changes in Quaternary environments (Ross and others, 1970; Ross and Degens, 1974; Hay, 1988; Hay and Honjo, 1989). The lowermost unit records sedimentation that occurred when eustatic sea levels were lower (7,000-25,000 B.P.) and the Black Sea was cut off from the Mediterranean Sea. Toward the end of this period the melting of ice introduced enough fresh water to make the Black Sea a freshwater lake and to transport large amounts of siliciclastics into the basin. Rising sea levels at the end of the Pleistocene increased the salinities and initiated the transition to the modern anoxic bottom water conditions. The sapropel of the middle unit was deposited under the brackish conditions present at that time. The upper unit is composed of Recent sediments (<3,000 B.P.) that were deposited under conditions similar to those now present (Ross and Degens, 1974).

The purpose of this report is to describe the X-ray mineralogy of some of these cores, to compare these results with analyses of nearby river sediment, and to comment on the factors controlling the distribution of sediments in the Black Sea.

METHODS

X-ray powder diffraction analyses were performed on 109 samples from 16 cores collected in the Black Sea and from 9 adjacent rivers (Fig. 1). A split from each sample was mounted as a randomly oriented powder and X-rayed. Semiquantitative estimates of the mineral abundances determined from the randomly oriented aggregate mounts were made by comparing the sample diffraction peak areas and intensities with the areas and intensities recorded from a collection of external standards. The clay fraction (<2 μm) from each sample was separated by centrifuge and mounted as an oriented aggregate on a glass slide by a filter-membrane peel technique (Pollastro, 1982). Each oriented clay mineral sample was subjected to four treatments (air-drying, glycolation with ethylene glycol, heating to 400 °C, and heating to 550 °C) to determine which clay minerals were present.

Clay mineral abundances were estimated by a method described by Biscaye (1965). The data from the randomly oriented and oriented aggregate mounts were combined. The semiquantitative estimates are reported in relative weight percentages of crystalline material and are generally considered to be accurate to within 10 percent of their actual values; however, even if due only to rounding errors, the lower values (<10 percent) may vary considerably more than this.

A split was taken from each sample and mounted in Piccolite (N=1.52) as a smear slide. The slides were used to check the semiquantitative diffraction results, to generate textural descriptions, to identify layered silicates occurring in the silt fraction, to detect amorphous phases or those occurring in trace amounts, and to examine the biogenic debris.

The mineralogical data for each sample are divided into two separate distributions: relative clay mineral abundances and whole sample mineralogy. The values in both data sets are in relative percent and normalized to 100%. A blank in the X-ray diffraction data tables indicates that the mineral was not detected; T indicates an occurrence of less than 1%.

X-RAY MINERALOGY

The results of the X-ray powder diffraction analyses are presented in the Tables 1-8; clay mineralogy alone is shown in Tables 5-8. In order to present two continuous undisturbed data profiles, cores from four adjacent sites. Box core 21 is listed with giant gravity core 19 in Tables 1 and 5, and box core 55 is listed with giant gravity core 38 in Tables 2 and 6. The remaining deep-water cores are presented in Tables 3 and 7. Results from the rivers are listed in Tables 4 and 8.

Layered silicates, which range in concentration from 7 to 75 percent of the samples, are always a major constituent of the siliciclastic portion of the Black Sea sediments. Illite consistently dominates the clay fraction throughout cores BC21, GGC-19, GGC-1, GGC-9, and BC-10 from the western Black Sea (Tables 5 and 7) and in the rivers discharging into the northwestern part of the Black Sea (Table 8). Smectites are usually more abundant in the upper varved portion of the sections (Unit 1) penetrated in the eastern Black Sea and in the rivers discharging into the south-central part of the Black Sea (Tables 6, 8). Although smectite is slightly more common than illite, these minerals alternate in zones of enrichment or occur in roughly equal amounts in the sapropels (Unit II) and lacustrine deposits at the core sites in the eastern Black Sea (Tables 6, 7).

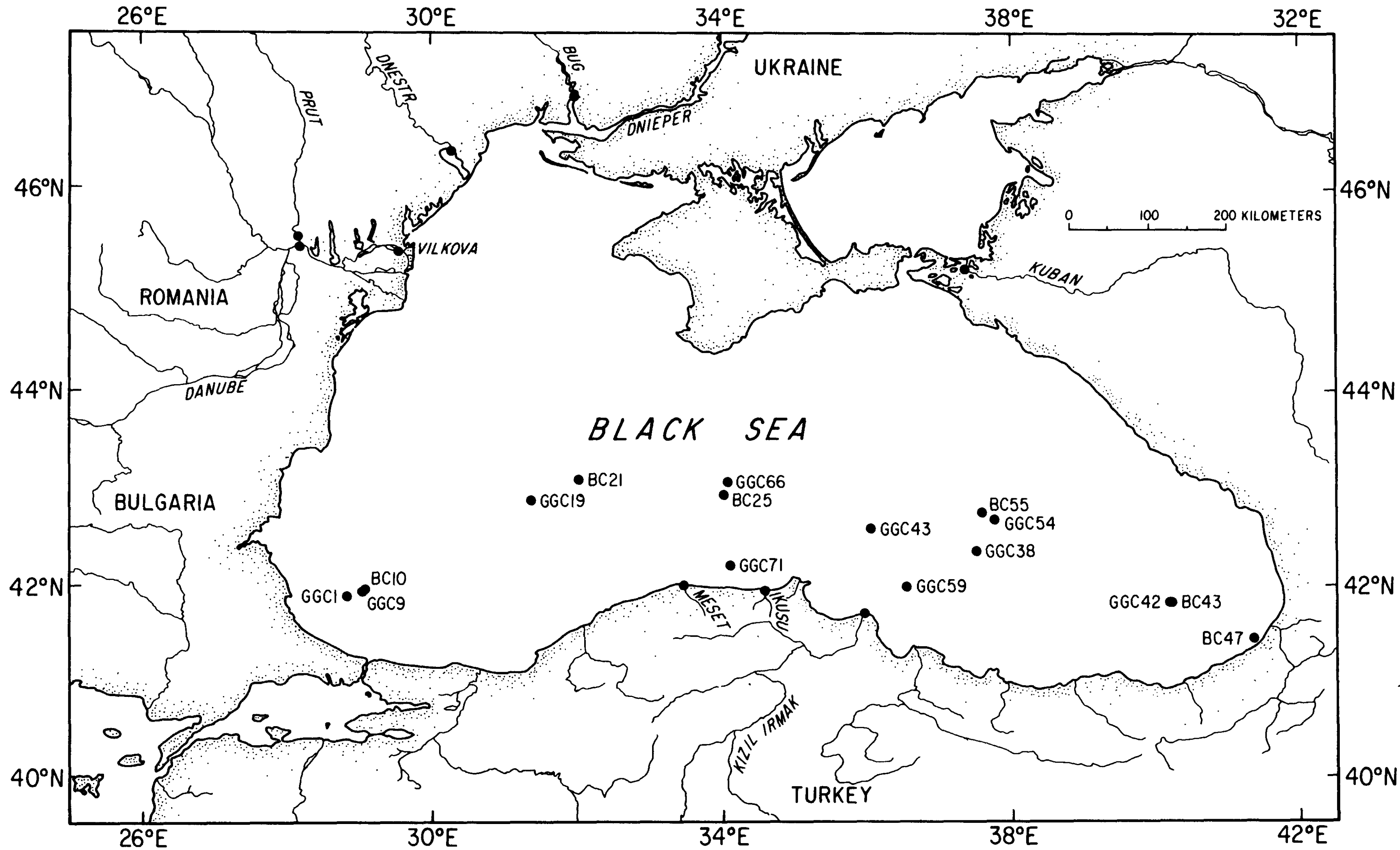

Figure 1. Map of the Black Sea showing the sample locations (solid circles).

Table 1. X-ray mineralogy of sediments in box core BC21 and giant gravity core GGC-19 from the southwestern Black Sea. The numbers separated from the core identifiers by a hyphen refer to depths (in centimeters) below the sediment-water interface. Values are in relative percent. T: trace; a blank indicates mineral not present.

SAMPLE	LAYERED SILICATES	QUARTZ	FELDSPAR	CALCITE	DOLOMITE	PYRITE
UNIT 1						
BC21-5	19	3		73		5
BC21-7	18	5	T	70		6
BC21-9	13	2		82		3
BC21-11	9	2	T	85		3
BC21-13	17	4	T	73		5
BC21-15	16	3	T	75		5
BC21-17	9	2		86		3
BC21-19	18	4	T	74		4
BC21-21	55	17	3	22		3
BC21-23	8	1	T	88		4
BC21-25	11	3		82		4
BC21-27	12	2		82		4
BC21-29	12	3	T	80		4
BC21-31	14	4	T	77		4
BC21-33	11	2	T	82		4
UNIT 2						
BC21-35	27	8	1	55		9
BC21-37	42	17	2	24	T	14
BC21-39	44	16	1	22	2	15
BC21-41	42	12	2	26	T	17
BC21-43	11	2	1	82		4
BC21-45	45	13	2	23	5	12
BC21-47	56	18	3	15	1	7
BC21-49	55	18	3	17	1	6
BC21-T	54	18	3	21	T	3
GGC19-45	57	15	4	15	T	8
GGC19-47	61	14	4	15	T	5
GGC19-49	52	14	3	17	4	10
GGC19-51	60	14	3	10	T	12
GGC19-53	64	14	4	14		4
GGC19-55	62	16	4	7	T	10
GGC19-57	58	15	3	11	T	12
UNIT 3						
GGC19-59	69	17	2	8	1	3
GGC19-61	68	19	3	7		3
GGC19-63	65	19	3	7	3	3
GGC19-65	75	16	4	4		1
GGC19-67	56	19	3	8	6	8
GGC19-69	57	17	4	9	4	9
GGC19-71	61	12	3	15	3	6
GGC19-73	57	18	3	15	3	4

Table 2. X-ray mineralogy of the sediments in box core BC55 and giant gravity core GGC38 from the southeastern Black Sea. The numbers separated from the sample identifiers by a hyphen refer to depths (in centimeters) below the sediment-water interface. Values are in relative percent. T: trace; a blank indicates mineral not detected.

SAMPLE	LAYERED SILICATES	QUARTZ	FELDSPAR	CALCITE	DOLOMITE	PYRITE
UNIT 1						
BC55-5	20	6	1	67		6
BC55-7	23	6	1	64		6
BC55-9	16	3	T	77		3
BC55-11	7	2		89		2
BC55-13	13	6	T	76	T	4
BC55-15	16	6	T	74		3
BC55-17	11	3	T	81		4
BC55-19	14	4	T	78		3
BC55-21	10	4	T	83		2
BC55-23	9	2		86	T	2
BC55-25	12	2	T	83	T	2
BC55-27	15	5	T	75	T	5
BC55-29	16	4	1	76		3
BC55-31	18	8	T	69		4
BC55-33	9	2		87		2
UNIT 2						
BC55-35	31	10	2	47	1	9
BC55-37	47	12	2	26	2	11
BC55-39	46	14	4	21	2	13
BC55-41	43	11	2	30	1	13
BC55-43	15	5	T	73		6
BC55-45	44	11	1	23	3	18
BC55-47	55	14	3	19	1	7
BC55-49	54	14	3	20	3	6
BC55-51	54	15	3	21	3	4
BC55-53	49	14	4	24	2	7
GGC38-45	58	13	4	14	1	10
GGC38-47	54	13	4	22	1	6
GGC38-49	58	12	4	16	1	9
GGC38-51	62	12	4	12	1	9
GGC38-53	56	15	4	15	1	9
GGC38-55	56	13	4	13	1	13
GGC38-57	61	16	3	11	T	8
UNIT 3						
GGC38-59	57	14	6	16	T	6
GGC38-61	71	15	4	5	T	4
GGC38-63	67	16	4	7	T	5
GGC38-65	58	12	6	15		9
GGC38-67	62	13	6	13		6
GGC38-69	59	17	4	9	3	8
GGC38-71	65	13	3	12		7

Table 3. X-ray mineralogy of sediments from cores in the southern Black Sea. Numbers separated from the sample identifiers refer to depths (in centimeters) below the sediment-water interface. Values are in relative percent. T: trace; a blank indicates mineral not detected.

SAMPLE	LAYERED SILICATES	QUARTZ	FELDSPAR	CALCITE	DOLOMITE	PYRITE
GGC1-8	46	13	3	33	1	4
GGC1-39	57	18	4	15	2	4
GGC1-49	59	15	4	8	7	7
GGC1-83	55	19	4	11	7	4
BC10-8	32	8	1	54	T	4
BC10-TURBIDITE	46	10	2	37	2	3
GGC9-12	57	16	4	12	6	4
GGC9-39	51	14	3	20	3	9
GGC9-40	60	19	3	8	7	3
BC25-8	33	9	1	52	T	4
BC25-39	54	14	3	16	6	7
BC25-49	57	16	6	10	6	5
BC25-TURBIDITE3	56	15	5	13	2	9
GGC66-65	61	16	4	12	3	4
BC43-8	42	11	3	37		7
GGC42-39	56	15	4	17	T	7
GGC42-49	53	16	8	13	T	9
GGC42-75	53	16	10	12		9
GGC42-TURBIDITE1	48	13	11	20	1	7
GGC59-39	56	14	5	13	T	9
GGC43-13	52	13	5	17	T	8
GGC43-79	54	16	6	13	1	10
GGC71-280-300	57	18	5	11	1	6
GGC71-640	53	20	6	11	1	5
GGC54-TURBIDITE	52	14	10	14	T	8
BC47-TOP	52	13	11	18	1	5
BC47-BOT	42	13	12	21	1	11

Table 4. X-ray mineralogy of sediment samples from rivers discharging into the Black Sea. Values are in relative percent. T: trace; a blank indicates mineral not detected.

SAMPLE	LAYERED SILICATES	QUARTZ	FELDSPAR	CALCITE	DOLOMITE	PYRITE
RUSSIAN RIVERS						
DANUBE						
VILKOVA	19	43	15	8	14	T
DANUBE	44	44	6	4	2	
PRUT	31	45	15	6	3	
DNESTR	38	50	6	4	2	
BUG	5	83	7	4	T	
KUBAN	48	36	12	4		
TURKISH RIVERS						
IKISU	28	20	7	45		
KIZIL IRMAK	47	19	12	18	4	
MESET	51	19	20	9	T	

Table 5. Clay mineralogy of the sediments in box core BC21 and giant gravity core GGC-19 from the southwestern Black Sea. The numbers separated from the core identifiers by a hyphen refer to depths (in centimeters) below the sediment-water interface. Values are in relative percent. T: trace; a blank indicates mineral not detected.

SAMPLE	SMECTITE	MIXED-LAYER	CHLORITE	ILLITE	KAOLINITE
UNIT 1					
BC21-5	32		11	45	12
BC21-7	21		13	52	14
BC21-9	27		10	50	12
BC21-11	23		13	51	13
BC21-13	32	T	11	45	11
BC21-15	34		10	45	11
BC21-17	26	T	11	49	14
BC21-19	37		11	43	10
BC21-21	26		11	51	12
BC21-23	24	T	12	52	11
BC21-25	27		12	50	11
BC21-27	32		10	45	13
BC21-29	28		11	46	15
BC21-31	31	T	10	46	12
BC21-33	28	T	11	46	14
UNIT 2					
BC21-35	41	T	8	42	8
BC21-37	36	T	9	42	12
BC21-39	29		8	48	15
BC21-41	31	2	11	43	13
BC21-43	22	2	13	52	11
BC21-45	27	2	13	45	13
BC21-47	15	2	10	61	12
BC21-49	35	T	9	44	11
BC21-T	26		14	48	12
GGC19-45	19	T	12	55	13
GGC19-47	18	2	13	56	12
GGC19-49	22	T	10	57	10
GGC19-51	24	T	10	55	10
GGC19-53	20		13	55	12
GGC19-55	26	2	12	51	9
GGC19-57	28	2	9	52	9
UNIT 3					
GGC19-59	25		12	53	10
GGC19-61	27	T	10	53	9
GGC19-63	23	2	17	47	12
GGC19-65	27		12	52	9
GGC19-67	23	T	11	55	10
GGC19-69	32		10	49	9
GGC19-71	34		12	44	10
GGC19-73	30		13	47	10

Table 6. Clay mineralogy of the sediments in box core BC55 and giant gravity core GGC38 from the southeastern Black Sea. The numbers separated from the core identifiers by a hyphen refer to the depth (in centimeters) below the sediment-water interface. Values are in relative percent. T: trace; a blank indicates mineral not detected.

SAMPLE	SMECTITE	MIXED-LAYER	CHLORITE	ILLITE	KAOLINITE
UNIT 1					
BC55-5	44	T	7	37	11
BC55-7	52		6	34	8
BC55-9	53	2	6	29	10
BC55-11	53	2	6	31	8
BC55-13	56		7	30	8
BC55-15	57	2	8	26	7
BC55-17	59	T	6	28	6
BC55-19	57		6	31	6
BC55-21	52		6	35	7
BC55-23	55	T	8	27	9
BC55-25	52		6	35	7
BC55-27	53		6	33	8
BC55-29	56	T	8	26	9
BC55-31	62		7	24	8
BC55-33	46	1	9	35	9
UNIT 2					
BC55-35	61		7	24	8
BC55-37	38		9	47	6
BC55-39	35	T	11	43	10
BC55-41	34	2	10	45	9
BC55-43	55		6	31	7
BC55-45	42		9	37	12
BC55-47	43	T	11	32	13
BC55-49	54	T	8	28	9
BC55-51	27	2	13	44	12
BC55-53	26	1	14	48	10
GGC38-45	36		14	37	13
GGC38-47	54		10	27	8
GGC38-51	50		12	28	10
GGC38-53	55	1	8	26	8
GGC38-55	40		13	35	12
GGC38-57	41	T	15	33	10
UNIT 3					
GGC38-59	45		13	31	11
GGC38-61	39	2	16	34	9
GGC38-63	33		15	40	11
GGC38-65	40		13	36	11
GGC38-67	43		14	33	9
GGC38-69	35		13	43	9
GGC38-71	39		14	36	11

Table 7. Clay mineralogy of sediments from cores in the southern Black Sea. Numbers at the end of the core identifier refer to depths (in centimeters) below the sediment water interface. Values are in relative percent. T: trace; a blank indicates mineral not detected.

SAMPLE	SMECTITE	MIXED-LAYER	CHLORITE	ILLITE	KAOLINITE
GGC1-8	25		10	56	9
GGC1-39	24		9	58	9
GGC1-49	31		9	53	7
GGC1-83	28		11	51	10
BC10-8	25	T	11	51	11
BC10-TURBIDITE	30		11	49	10
GGC9-39	34		10	46	10
GGC9-12	33		9	49	9
GGC9-40	21	T	9	60	9
BC25-8	34	T	8	48	9
BC25-39	34		10	48	8
BC25-49	26		9	57	8
BC25-TURBIDITE	48		11	32	9
GGC66-65	32	T	9	47	11
BC43-8	34		12	41	13
GGC42-39	35		12	43	10
GGC42-75	29		17	39	15
GGC42-TURBIDITE	34		16	37	13
GGC59-39	34		12	45	9
GGC43-13	36		14	39	11
GGC43-79	41		12	38	9
GGC71-280/300	32		11	49	6
GGC71-640	41		9	43	7
GGC54-TURBIDITE	26		18	43	13
BC47-Top	29	T	29	33	8
BC47-Bot	29		30	31	10

Table 8. Clay mineralogy of sediment samples from rivers discharging into the Black Sea. Values are in relative percent. T: trace; blanks indicate mineral not detected.

SAMPLE	SMECTITE	MIXED-LAYER	CHLORITE	ILLITE	KAOLINITE
RUSSIAN RIVERS					
DANUBE					
VILKOVA	27		11	53	9
DANUBE	27		8	61	5
PRUT	29	T	10	54	6
DNESTR	32		7	56	5
BUG	29	T	7	50	14
KUBAN	33		13	35	19
TURKISH RIVERS					
IKISU	48		10	39	3
KIZIL IRMAK	43	T	19	26	12
MESET	65		8	25	2

Small amounts of mixed-layer illite-smectite occur sporadically throughout the cores.

Kaolinite, which usually forms by chemical weathering under nonalkaline conditions, is slightly more common than chlorite in Unit I of the eastern Black Sea. Chlorite is more common than kaolinite in Units 2 and 3 in both the eastern and western Black Sea and in the modern river sediment analyzed during this study. Together both minerals comprise a greater portion of the layered silicate fraction in the western Black Sea and in the sapropels and lacustrine deposits of the eastern Black sea. No mixed-layer chlorite-smectite or zeolites were detected in any of the X-ray diffraction patterns.

Quartz grains are present in every sample (Tables 1, 2, 3, and 4); they range in size from very fine sand to fine silt. Although potassium feldspar is occasionally present in trace amounts, plagioclase is the dominant feldspar in all of the samples.

Calcite (low-magnesium) is common throughout the cores as both biogenic debris in the varves of coccolith ooze in the upper layer and as an authigenic precipitate and detrital component in the underlying sediments. The sapropels and lacustrine deposits contain much less biogenic calcite and, consequently, much less carbonate. The dolomite (ankerite?), which is authigenic and occurs as silt-sized euhedral rhombs, is more common in the sapropel (Unit 2). Faint peaks at 3.40 angstroms in the X-ray diffraction patterns suggest that traces of aragonite may also be present in the upper layer.

Although pyrite is common throughout the Black Sea sediments owing to the anoxic interstitial environment, the organic-rich sapropels (Unit 2) are quite pyritic. The pyrite, which ranges up to 18 percent in the sapropels, occurs chiefly as silt-sized framboidal spheres. Rapid color changes reported in shipboard sampling logs suggest that monosulfides are also present (Honjo and Hay, 1988).

COMMENTS

Generally, our results on the mineralogy of the varved upper layer (Unit 1) are similar to those reported during an earlier study of surficial sediments in the Black Sea (Muller and Stoffers, 1974). However, our results show lower quartz/feldspar ratios and less dolomite than this earlier study.

Mineralogical differences in the siliciclastic sediments between the southwestern and southeastern parts of the Black Sea are related to provenance. For example, illite is the dominant clay mineral in the Danube, Dnestr, and Bug rivers. These rivers discharge into the western Black Sea and apparently control terrigenous sedimentation. Conversely, smectite is the dominant clay mineral in the Meset, Ikusu, and Kizil Irmak rivers of Turkey. These rivers discharge across a relatively narrow shelf (Ross and Degens, 1974) into the south-central part of the Black Sea and, therefore, influence modern sedimentation there.

The greater abundance of illite in the sediments of Units 2 and 3 in the southeastern Black Sea (relative to the amount of illite in the upper varved layer) suggests that depositional patterns were different during the Late Pleistocene and early Holocene. During this time sediment-laden rivers were swollen by glacial meltwaters. Coupled with a lower sea level (Deuser, 1974), these conditions probably allowed more of the sediment in the large rivers of the northwest to escape the estuaries, cross the broad shelf present in this area, and make it into the deep southeastern basin.

REFERENCES

Biscaye, P.E., 1965, Mineralogy and sedimentation of Recent deep-sea clay in the Atlantic Ocean and adjacent seas and oceans: Geological Society America Bulletin, v. 76, no. 7, p. 803-832.

Deuser, W.G., 1974, Evolution of anoxic conditions in Black Sea during Holocene: In E.T. Degens and D.A. Ross (Editors), The Black Sea - Geology, Chemistry, and Biology, American Association of Petroleum Geologists Memoir 20, p. 133-143.

Hay, B.J., 1988, Sediment accumulation in the central and western Black Sea over the past 5100 years: Paleoceanography, v. 3, p. 491-508.

Hay, B.J. and Honjo, S., 1989, Particle deposition in the present and Holocene Black Sea: Oceanography, v. 2, p. 26-31.

Honjo, S. and Hay, B.J., 1988, Temporal and spatial variability in sedimentation in the Black Sea: Woods Hole Technical Report 88-35, 156 p.

Muller, G. and Stoffers, P., 1974, Mineralogy and Petrology of Black sea sediments: In E.T. Degens and D.A. Ross (Editors), The Black Sea - Geology, Chemistry, and Biology, American Association of Petroleum Geologists Memoir 20, p. 200-248.

Pollastro, R.M., 1982, A recommended procedure for the preparation of oriented clay-mineral specimens for X-ray diffraction analysis -modifications to Dever's filter-membrane peel technique: U.S. Geological Survey Open-File Report 82-71, 10 p.

Ross, D.A., Degens, E.T., and MacIlvaine, J., 1970, Black Sea - Recent sedimentary history: Nature, v. 170, p. 163-165.

Ross, D.A. and Degens, E.T., 1974, Recent sediments of the Black Sea: In E.T. Degens and D.A. Ross (Editors), The Black Sea - Geology, Chemistry, and Biology, American Association of Petroleum Geologists Memoir 20, p. 183-199.

Shimkus, K.M. and Trimonis, E.S., 1974, Modern sedimentation in the Black Sea: In E.T. Degens and D.A. Ross (Editors) The Black Sea - Geology, Chemistry, and Biology, American Association of Petroleum Geologists Memoir 20, p. 249-278.